AUT Journal of Modeling and Simulation

AUT J. Model. Simul., 55(1) (2023) 183-198
DOI: 10.22060/miscj.2023.22582.5332

A Robust Self-contained Solution for Inertial Attitude Determination Under External Acceleration

M.A. Amiri Atashgah[1], M. Ebrahimi Dormiani[1] ,H. Mohammadkarimi[2]

[1] Faculty of New Sciences and Technologies, University of Tehran, Tehran, Iran.
[2]Department of Aerospace Engineering, Amirkabir University of Technology, Tehran, Iran.

ABSTRACT: One of the main issues in inertial navigation systems is attitude determination, which means estimating the level angles (i.e., roll and pitch). This paper investigates the attitude estimation problem for an accelerated rigid body using three gyros and three accelerometers. The most critical challenges in attitude determination systems are external accelerations and gyroscope drift errors. Thus, a novel method based on the adaptive filter-Kalman algorithm is proposed to estimate and compensate for these errors. Linearization was performed around a general work point, and the covariance matrix's adaptive values were obtained so that leveling angles were accurately determined despite external accelerations. The simulation results, along with the car test, which was performed in different dynamic conditions with external accelerations, showed that the introduced algorithm has a high capability in accurately estimating leveling angles. This approach can be used for GPS-less navigation Algorithms.

Review History:

Received: Jul. 27, 2023
Revised: Sep. 23, 2023
Accepted: Oct. 09, 2023
Available Online: Oct. 10, 2023

Keywords:

Attitude Determination
Adaptive Kalman Filtering
Inertial Navigation System
Attitude and heading Reference System
Self-contained Navigation Algorithm

1- Introduction

An inertial navigation system typically uses three orthogonal accelerometers and three orthogonal gyroscopes that form an Inertial Measurement Unit (IMU) assembly. By integrating the output of an IMU, it is possible to derive all the navigation parameters, such as position, speed, and attitude of a moving vehicle. Determining the attitude of a vehicle is equal to determining the Euler angles (i.e., roll, pitch, and yaw). In this study, the purpose is to determine the level angles, which are the roll and pitch angles of a vehicle.

Estimation of attitude includes two phases: 1) estimation of attitude from measurements and sensors and 2) filtering of measurement noises. The second phase can be completed by combining measurements and models, where the modeling is done with different methods. For instance, consider a model with a three-axis rate gyroscope whose value is affected by noise; It is required to take new states into account in addition to the system states to determine the gyro's drift. In this situation, a technique known as the 'complementing method' (such as Madgwick and Mahony methods) is applied [1-3]. In this method, the gyroscope's output is used to filter the noise from the measurement, and the measurement is applied to determine the deviation of the gyroscope. Due to their simplicity and light computational loads, complimentary filters are typically employed in devices like mobile phones and smartwatches. Sometimes, an adaptive approach is utilized to improve the accuracy of complementary filters; For example, by detecting the location of a mobile phone and modifying the gain of an accelerometer in each axis, it is feasible to obtain a better calculation of level angles [4].

One of the most useful filters for attitude determination is the Extended Kalman filter (EKF) [5-11]. In some state determination applications, an advanced form of EKF called Multiplicative EKF (MEKF) is used [9, 11]. The linearization process that occurs in EKF, causes a reduction in the performance of this filter. Numerous studies have been performed to develop these filters; These studies have used the basic structure of EKF, including incremental EKF method [12-17], recursive EKF [18], quasi-deterministic EKF [19-21], and a two-stage optimal EKF [22].

One of the essentials for designing filters and observers in determining the attitude is using adaptive methods. Filters developed in this way are generally divided into two groups: The first group is filters that adjust the values of dynamic covariance, measurement covariance, or both, in the Kalman filters adaptively [23, 24]. Also, some filters have been designed to work with colored and white noises in an adaptive manner [25]. Additionally, in [26, 27] an adaptive

*Corresponding author's email: h.mohammadkarimi@aut.ac.ir

filter is introduced to deal with the uncertainty in dynamic noise modeling. The second group is filters that adaptively estimate the uncertain parameters of the system, such as the inertia matrix, or other constant parameters such as biases [28-30]. In [31], the perturbations related to the angular rate were considered as functions of biases and estimated using an adaptive filter.

Several mechanizations for attitude determination have been proposed and reviewed in .[32-34] There isn't a single mechanization that can be generally favored above the others [35]. Among all the filters, the Discrete Kalman Filter (EKF) is the most widely used type in real-time state determination problems. Although new challenges such as singularity and non-continuity appeared in EKF, this filter found an outstanding performance in most applications of attitude determination [36, 37].

Reference [38] proposes an enhanced attitude and heading reference system (AHRS) algorithm specifically designed for unmanned aerial vehicles (UAVs). The algorithm utilizes a particle filter, a probabilistic estimation technique, to enhance the accuracy of attitude estimation. By incorporating measurements from accelerometers, gyroscopes, and magnetometers, the algorithm effectively combines sensor data to estimate the UAV's attitude with improved accuracy. The proposed algorithm addresses the challenges of UAV dynamics and sensor measurement errors, making it suitable for applications requiring precise attitude estimation for UAV control and navigation.

Reference [39] presents a novel inertial navigation system that utilizes a low-cost MEMS (Micro-Electro-Mechanical Systems) AHRS. The system combines accelerometer and gyroscope data from the MEMS AHRS with an inertial navigation algorithm to estimate position, velocity, and attitude. The proposed system offers a cost-effective solution for navigation applications that require accurate position and orientation estimation.

Reference [40] introduces an adaptive unscented Kalman filter (AUKF) to enhance the attitude estimation accuracy of MEMS-based AHRS. By adaptively adjusting the process and measurement noise covariance matrices, the AUKF algorithm can effectively mitigate the impact of sensor errors and environmental disturbances. The proposed approach improves the robustness and accuracy of attitude estimation for AHRS applications.

Reference [41] presents a novel adaptive unscented Kalman filter (AUKF) with fading memory for robust attitude estimation in AHRS. The proposed filter dynamically adjusts its fading memory parameter based on the current sensor measurement noise level, enabling adaptive estimation and improved performance in varying conditions. The experimental results demonstrate the effectiveness of the proposed approach in enhancing AHRS accuracy and robustness.

Reference [42] presents an attitude estimation method for AHRS based on the Mahony filter and adaptive notch filter. The Mahony filter is employed to fuse sensor data and estimate attitude, while the adaptive notch filter is utilized to remove noise and interference caused by vibrations. The proposed approach improves the accuracy of AHRS attitude estimation, particularly in environments with high-frequency vibrations.

Reference [43] addresses the optimization problem of the attitude and heading reference system (AHRS). It formulates the AHRS problem as a nonlinear optimization task and explores various optimization techniques to obtain the best estimates of attitude and heading. The study investigates the performance of different optimization algorithms and provides insights into improving AHRS estimation accuracy.

Reference [44] proposes an AHRS correction algorithm based on a radial basis function (RBF) neural network for underwater autonomous underwater vehicles (AUVs). The algorithm aims to compensate for the dynamic errors caused by sensor biases and disturbances in underwater environments. By utilizing the RBF neural network, the proposed algorithm achieves accurate attitude estimation and improves the navigation performance of AUVs.

Reference [45] presents a quaternion-based adaptive unscented Kalman filter (AUKF) for AHRS with biased rate gyroscopes. The proposed filter combines quaternions, which represent attitude, with an adaptive estimation approach to handle the bias errors in rate gyro measurements. The algorithm adapts the filter gain and covariance matrices to improve attitude estimation accuracy and mitigate the effects of biased sensors.

Reference [46] presents a robust AHRS attitude complementary filter algorithm based on a nonlinear parameter fading extended Kalman filter (EKF). The algorithm combines the strengths of a complementary filter and an EKF to estimate attitude, while the nonlinear parameter fading technique adapts the filter to changing conditions. The proposed algorithm enhances AHRS robustness against measurement noise and external disturbances.

Reference [47] proposes an adaptive unscented Kalman filter (AUKF) algorithm for the attitude and heading reference system. The algorithm adaptively adjusts the filter parameters based on the measurement noise covariance and updates the filter gain matrix to improve estimation accuracy. The experimental results demonstrate the effectiveness of the proposed algorithm in enhancing the performance of the AHRS in terms of attitude and heading estimation.

One of the approaches that are used in attitude determination algorithms is to adjust the covariance matrix of the measurement error based on the acceleration limits (zero, low, and high acceleration) in different maneuvers [48, 49]. This method has some problems in rotating maneuvers. Since one of the challenges in determining the attitude is the existence of external acceleration, several researchers have attempted to counteract this effect by estimating the amount of external acceleration [50]; However, this method leads to a significant error in estimating level angles in fast maneuvers.

By studying and examining the results of numerous experimental tests carried out in static and dynamic conditions, it was concluded that two factors are very important in

adapting the attitude determination algorithm: the first factor is the rapid detection of the maneuver change from static to dynamic condition. The second factor is determining the value of the error covariance matrix according to the dynamic conditions of the vehicle. In most references, such as [51-55], one of these two cases is considered; In this paper, both factors are considered together and a new method based on the adaptive estimator is introduced which improves the accuracy of attitude determination.

The organization of this paper is as follows: In section 2, mathematical modeling of the attitude determination algorithm is presented. In section 3, by linearizing the rotational kinematics of a rigid body, the discrete equations of the problem is obtained to be applied in a Kalman filter. In section 4, numerical simulation is carried out in MATLAB software. In section 5, a car test is performed to validate the algorithm and the results are presented.

2- Kinematic modeling

In this section, fundamental relations that determine the level angles are presented. According to Newton's second law we have:

$$\mathrm{m}^{\mathrm{B}}\mathrm{D}^{\mathrm{I}}\mathbf{v}_{\mathrm{B}}^{\mathrm{I}} = \mathbf{f}_{\mathrm{a}} + \mathbf{f}_{\mathrm{p}} + \mathrm{m}^{\mathrm{B}}\mathbf{g} \tag{1}$$

Where I is the inertial frame, m^{B} is the mass of the vehicle, D^{I} is the rotational time derivative relative to the inertial frame, $\mathbf{v}_{\mathrm{B}}^{\mathrm{I}}$ is the velocity of the body frame with respect to the inertial frame, $\mathbf{f}_{\mathrm{a}}$ and $\mathbf{f}_{\mathrm{p}}$ are the aerodynamic and propulsive force vector and $\mathbf{g}$ is the gravitational acceleration. If the external force acting on the vehicle is written as $\mathbf{f}_{\mathrm{ext}} = \mathbf{f}_{\mathrm{a}} + \mathbf{f}_{\mathrm{p}}$, equation (1) can be written as:

$$\mathrm{m}^{\mathrm{B}}\mathrm{D}^{\mathrm{I}}\mathbf{v}_{\mathrm{B}}^{\mathrm{I}} = \mathbf{f}_{\mathrm{ext}} + \mathrm{m}^{\mathrm{B}}\mathbf{g} \rightarrow \mathrm{D}^{\mathrm{I}}\mathbf{v}_{\mathrm{B}}^{\mathrm{I}} = \frac{\mathbf{f}_{\mathrm{ext}}}{\mathrm{m}^{\mathrm{B}}} + \mathbf{g} \tag{2}$$

In equation (2), the D^{I} the operator can be shifted to the D^{B} operator as follows [56]:

$$\begin{aligned} &\mathrm{D}^{\mathrm{B}}\mathbf{v}_{\mathrm{B}}^{\mathrm{I}} + \boldsymbol{\Omega}^{\mathrm{BI}}\mathbf{v}_{\mathrm{B}}^{\mathrm{I}} = \frac{\mathbf{f}_{\mathrm{ext}}}{\mathrm{m}^{\mathrm{B}}} + \mathbf{g} \rightarrow \\ &\mathrm{D}^{\mathrm{B}}\mathbf{v}_{\mathrm{B}}^{\mathrm{I}} = \frac{\mathbf{f}_{\mathrm{ext}}}{\mathrm{m}^{\mathrm{B}}} + \mathbf{g} - \boldsymbol{\Omega}^{\mathrm{BI}}\mathbf{v}_{\mathrm{B}}^{\mathrm{I}} \end{aligned} \tag{3}$$

where D^{B} is the rotational time derivative relative to the body frame. Expressing equation (3) in the body frame results in:

$$\left[\mathrm{D}^{\mathrm{B}}\mathbf{v}_{\mathrm{B}}^{\mathrm{I}}\right]^{\mathrm{B}} = \frac{[\mathbf{f}_{\mathrm{ext}}]^{\mathrm{B}}}{\mathrm{m}^{\mathrm{B}}} + [\mathrm{T}]^{\mathrm{BG}}[\mathbf{g}]^{\mathrm{G}} - [\boldsymbol{\Omega}^{\mathrm{BI}}]^{\mathrm{B}}\left[\mathbf{v}_{\mathrm{B}}^{\mathrm{I}}\right]^{\mathrm{B}} \tag{4}$$

where

$$\begin{aligned} &[\mathrm{T}]^{\mathrm{BG}} = \begin{bmatrix} \cos\psi\cos\theta & \sin\psi\cos\theta & -\sin\theta \\ \cos\psi\sin\theta\sin\phi - \sin\psi\cos\phi & \sin\psi\sin\theta\sin\phi + \cos\psi\cos\phi & \cos\theta\sin\phi \\ \cos\psi\sin\theta\cos\phi + \sin\psi\sin\phi & \sin\psi\sin\theta\cos\phi - \cos\psi\sin\phi & \cos\theta\cos\phi \end{bmatrix} \\ &\left[\mathrm{D}^{\mathrm{B}}\mathbf{v}_{\mathrm{B}}^{\mathrm{I}}\right]^{\mathrm{B}} = [\dot{u} \quad \dot{v} \quad \dot{w}]^{\mathrm{T}} \\ &[\mathbf{g}]^{\mathrm{L}} = [0 \quad 0 \quad -\mathrm{g}]^{T} \\ &[\boldsymbol{\Omega}^{\mathrm{BI}}]^{\mathrm{B}} = \begin{bmatrix} 0 & -r & q \\ r & 0 & -p \\ -q & p & 0 \end{bmatrix} \end{aligned} \tag{5}$$

In equation (5), ϕ and θ are roll and pitch angles, respectively; ψ is the heading angle; u, v, and w are the components of linear velocity in the body frame; and p, q, and r are the components of angular velocity in the body frame. Inserting equation (5) into equation (4), the final form of the translational equation will be obtained:

$$\begin{aligned} \dot{u} &= a_{\mathrm{x}} + \mathrm{g}\sin\theta - (qw - rv) \\ \dot{v} &= a_{\mathrm{y}} - \mathrm{g}\cos\theta\sin\phi - (ru - pw) \\ \dot{w} &= a_{\mathrm{z}} - \mathrm{g}\cos\theta\cos\phi - (pv - qu) \end{aligned} \tag{6}$$

According to equation (6), the level angles are obtained as follows:

$$\begin{aligned} &\sin^{-1}\left(\frac{\dot{u} - a_x + qw - rv}{g}\right) \approx \sin^{-1}\left(\frac{-a_x}{g}\right) \\ &: \tan^{-1}\left(\frac{\dot{v} - a_y + ru - pw}{\dot{w} - a_z + pv - qu}\right) \approx \tan^{-1}\left(\frac{a_y}{a_z}\right) \end{aligned} \tag{7}$$

In Equation (7), when the GPS signal is available, the term equal is used and when the GPS signal is not available, the term approximately equal is used. It should be mentioned that the accuracy of attitude measurements is reduced in accelerated movement. This act accrues because the tilt measurements are accurate in cruise conditions; Thus, as the carrier deviates from this condition, the accuracy of the tilt measurements reduces.

3- Estimation Algorithm

The Discrete Kalman Filter (DKF) is one of the most widely used estimators in the field of navigation. In this research, DKF is used to determine the level angles. In the proposed algorithm, attitude propagation is based on the Euler method. The Eeuler approach is used due to the physical understanding of the level angles and the ease of tuning the corresponding coefficients of the DKF.

To start the algorithm, the initial value of the state vector and the error covariance matrix of the DKF should be determined. The flowchart of the DKF is shown in Figure 1; It has two main parts: the time update part and the measurement update part.

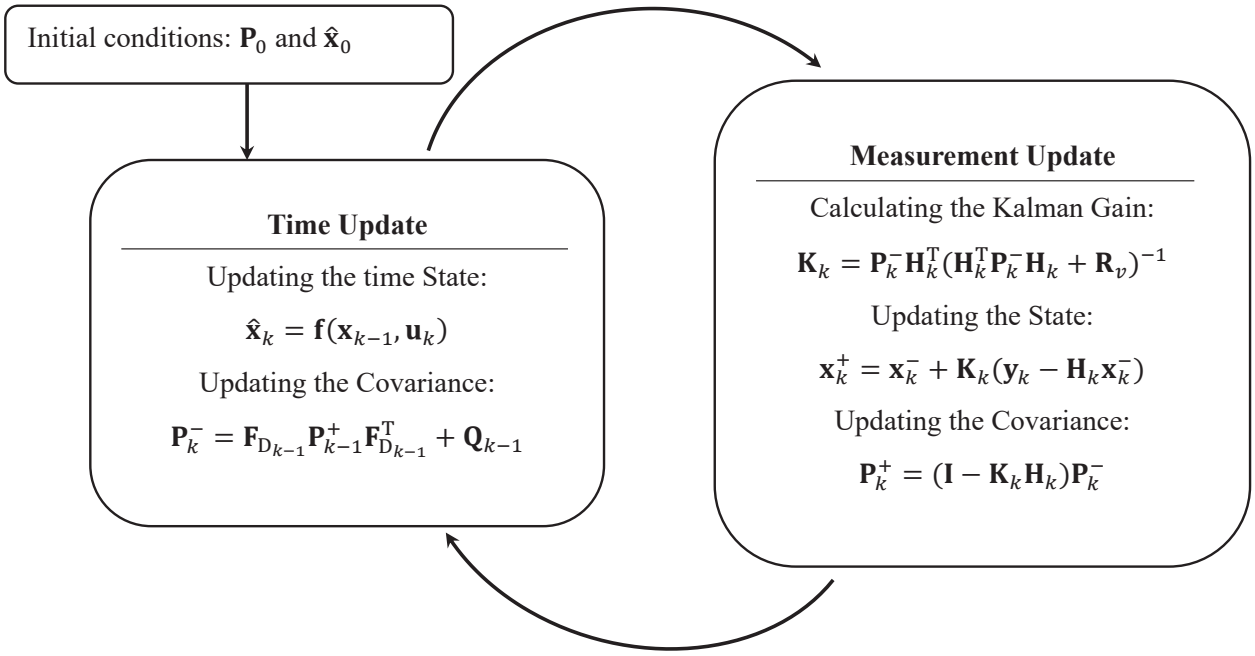

Fig. 1. Discrete Kalman filter flowchart

The different parts of the above flowchart in the attitude determination problem are explained in the following.

A- Initial conditions

The initial value of the level angles is determined as:

$$\theta_0 = \sin^{-1}\left(\frac{\dot{u} - a_{\mathrm{x}} + qw - rv}{g}\right)\Big|_{t=0} \approx \sin^{-1}\left(\frac{-a_{\mathrm{x}}}{g}\right)\Big|_{t=0}$$
$$\phi_0 = \tan^{-1}\left(\frac{\dot{v} - a_{\mathrm{y}} + ru - pw}{\dot{w} - a_{\mathrm{z}} + pv - qu}\right)\Big|_{t=0} \approx \tan^{-1}\left(\frac{a_{\mathrm{y}}}{a_{\mathrm{z}}}\right)\Big|_{t=0} \quad (8)$$

B- Time update

For determining the level angles, the following state vector is chosen in DKF:

$$\mathbf{x} = [\theta \quad \phi]^{\mathrm{T}} \quad (9)$$

The time update of the states is done by the Euler propagation method:

$$\dot{\theta} = cos\,\phi\, q - sin\,\phi\, r$$
$$\dot{\phi} = p + sin\,\phi\, tan\,\theta\, q + cos\,\phi\, tan\,\theta\, r \quad (10)$$

The system dynamics described by equation (10) is non-linear; DKF needs the linear form of this equation. The linearized form of equation (10), around the previous working point and in the state space will be as follows:

$$\delta\mathbf{x} = [\delta\theta \quad \delta\phi]^T \quad (11)$$

$$\delta\dot{\mathbf{x}} = \mathbf{F}_{\mathrm{c}}\delta\mathbf{x} + \mathbf{L}_{\mathrm{c}}\mathbf{w} \quad (12)$$

$$\mathbf{F}_{\mathrm{c}} = \begin{bmatrix} 0 & -(q\sin\phi + r\cos\phi) \\ \sec^2\theta(q\sin\phi + r\cos\phi) & \tan\theta(q\cos\phi - r\sin\phi) \end{bmatrix} \quad (13)$$

$$\mathbf{w} = [\delta p \quad \delta q \quad \delta r]^T \rightarrow \begin{cases} \delta p = \tilde{p} - p \\ \delta q = \tilde{q} - \mathrm{q} \\ \delta r = \tilde{r} - r \end{cases} \quad (14)$$

$$\mathbf{L}_{\mathrm{c}} = \begin{bmatrix} 0 & \cos\phi & -\sin\phi \\ 1 & \sin\phi\tan\theta & \cos\phi\tan\theta \end{bmatrix} \quad (15)$$

Also, the process noise, $\mathbf{Q}_{\mathrm{c}}$, is considered as follows:

$$\mathbf{Q}_{\mathrm{c}} = \mathrm{E}\{\mathbf{w}\mathbf{w}^{\mathrm{T}}\} = \begin{bmatrix} \sigma_{\mathrm{p}}^2 & 0 & 0 \\ 0 & \sigma_{\mathrm{q}}^2 & 0 \\ 0 & 0 & \sigma_{\mathrm{r}}^2 \end{bmatrix} \tag{16}$$

In equation (16), the elements on the main diagonal of the matrix are the variance of the measurement error of the gyroscopes and depend on the quality of the sensors. Also, The estimation error covariance is propagated as follows:

$$\mathbf{P}_k^- = \mathbf{F}_{\mathrm{D}_{k-1}} \mathbf{P}_{k-1}^+ \mathbf{F}_{\mathrm{D}_{k-1}}^{\mathrm{T}} + \mathbf{Q}_{k-1} \tag{17}$$

where $\mathbf{P}_k^-$ is the time-updated error covariance matrix at time step k; $\mathbf{P}_{k-1}^+$ is the measurement-updated error covariance matrix at time step k-1. Also, $\mathbf{Q}_k$ is the discretized equivalent of the continuous process noise, $\mathbf{Q}_{\mathrm{c}}$.

$$\mathbf{Q}_k = \mathbf{Q}_{\mathrm{c}} \Delta \mathrm{t}_k \tag{18}$$

Similarly, the matrix $\mathbf{F}_{\mathrm{D}_k}$ is the discretized equivalent of the continuous system matrix, $\mathbf{F}_{\mathrm{c}}$, and is calculated as follows [47]:

$$\mathbf{F}_{\mathrm{D}_k} = \exp(\mathbf{F}_{\mathrm{c}} \Delta \mathrm{t}_k) = \mathbf{I} + \mathbf{F}_{\mathrm{c}} \Delta \mathrm{t}_k + \frac{1}{2!}(\mathbf{F}_{\mathrm{c}} \Delta \mathrm{t}_k)^2 + \frac{1}{3!}(\mathbf{F}_{\mathrm{c}} \Delta \mathrm{t}_k)^3 + \cdots \tag{19}$$

C- Measurement Update

The measurement model is considered as follows:

$$\mathbf{y}_k = \tilde{\mathbf{y}}_k = [\tilde{\theta} \quad \tilde{\phi}]^T = \mathbf{H}_k \mathbf{x}_k + \mathbf{v}$$
$$\mathbf{H}_k = \mathbf{H} = \begin{bmatrix} 1 & 0 \\ 0 & 1 \end{bmatrix} \tag{20}$$

where $\mathbf{y}_k$ is the measurement vector and $\mathbf{H}$ is the measurement matrix; $\mathbf{x}_k$ is the state vector, and $\mathbf{í}$ is the measurement noise covariance:

$$\mathbf{v} \sim \mathrm{N}(\mathbf{0}, \mathbf{R}_{\mathrm{v}}) \tag{21}$$

The Kalman gain matrix, $\mathbf{K}_k$, is calculated as57]]:

$$\mathbf{K}_k = \mathbf{P}_k^- \mathbf{H}_k^{\mathrm{T}} (\mathbf{H}_k^{\mathrm{T}} \mathbf{P}_{\mathrm{k}}^- \mathbf{H}_k + \mathbf{R}_{\mathrm{v}})^{-1} \tag{22}$$

Utilizing the Kalman gain, The posterior covariance matrix and the state vector are updated as follows:

$$\mathbf{P}_k^+ = (\mathbf{I}_{2\times 2} - \mathbf{K}_k \mathbf{H}_k) \mathbf{P}_k^- \tag{23}$$

$$\delta \mathbf{x}_k^+ = \mathbf{K}_k (\tilde{\mathbf{y}}_k - \mathbf{H} \mathrm{x}_k^-) = \mathbf{K}_k (\tilde{\mathbf{y}}_k - \hat{\mathbf{y}}_k)$$
$$\mathbf{x}_k^+ = \mathbf{x}_k^- + \delta \mathbf{x}_k^+ \tag{24}$$

4- The adaptive law of attitude determination system

The attitude determination system must be able to estimate the Euler angles in different scenarios There are different motion phases for a moving vehicle where it experiences different angular and linear accelerations. In this study, an adaptive approach is used to adjust the measurement error covariance matrix by the change of vehicle motion behavior.

When the vehicle is in the non-accelerating phase, the measurements presented in equation (7) lead to a proper estimation of the alignment angles; However, if the device is under dynamic accelerations, the estimate of level angles is not accurate enough. The adaptation algorithm, utilizes the output of accelerometers and gyros to correct the covariance matrix of the measurement error automatically. This problem is achieved by separating the effects of acceleration components applied to the device. The analysis of these effects can be done based on Newton's second law; Which has the following form in the inertial frame:

$$\mathrm{m}^{\mathrm{B}} \mathrm{D}^{\mathrm{I}} \mathrm{D}^{\mathrm{I}} \mathbf{s}_{\mathrm{BI}} = \mathbf{f} \tag{25}$$

Expressing equation (25) with respect to the body frame, we would have:

$$\mathrm{m}^{\mathrm{B}} \mathrm{D}^{\mathrm{B}} \mathrm{D}^{\mathrm{B}} \mathbf{s}_{\mathrm{BI}} + \mathrm{m}^{\mathrm{B}} (\mathrm{D}^{\mathrm{B}} \boldsymbol{\Omega}^{\mathrm{BI}}) \mathbf{s}_{\mathrm{BI}} + 2\mathrm{m}^{\mathrm{B}} \boldsymbol{\Omega}^{\mathrm{BI}} (\mathrm{D}^{\mathrm{B}} \mathbf{s}_{\mathrm{BI}}) + \mathrm{m}^{\mathrm{B}} \boldsymbol{\Omega}^{\mathrm{BI}} \boldsymbol{\Omega}^{\mathrm{BI}} \mathbf{s}_{\mathrm{BI}} = \mathbf{f}_{\mathrm{ng}} + \mathrm{m}^{\mathrm{B}} \mathbf{g} \tag{26}$$

where $\mathbf{f}_{\mathrm{ng}}$ is the resultant non-gravitational forces, which can be measured by the accelerometers, and $\mathbf{s}_{\mathrm{BI}}$ is the position vector of the body frame concerning the inertial frame. Equation (26) could be rewritten as follows:

$$\tilde{\mathbf{a}} = \frac{\mathbf{f}_{\mathrm{ng}}}{\mathrm{m}^{\mathrm{B}}} = -\mathbf{g} + \begin{Bmatrix} +2\boldsymbol{\Omega}^{\mathrm{BI}} (\mathrm{D}^{\mathrm{B}} \mathbf{s}_{\mathrm{BI}}) & \text{coriolis acceleration} \\ +\boldsymbol{\Omega}^{\mathrm{BI}} \boldsymbol{\Omega}^{\mathrm{BI}} \mathbf{s}_{\mathrm{BI}} & \text{centrifugal acceleration} \\ +(\mathrm{D}^{\mathrm{B}} \boldsymbol{\Omega}^{\mathrm{BI}}) \mathbf{s}_{\mathrm{BI}} & \text{angular acceleration} \\ +\mathrm{D}^{\mathrm{B}} \mathrm{D}^{\mathrm{B}} \mathbf{s}_{\mathrm{BI}} & \text{linear acceleration} \end{Bmatrix}$$
$$+\mathbf{v} = -\mathbf{g} + \boldsymbol{\varepsilon} \tag{27}$$

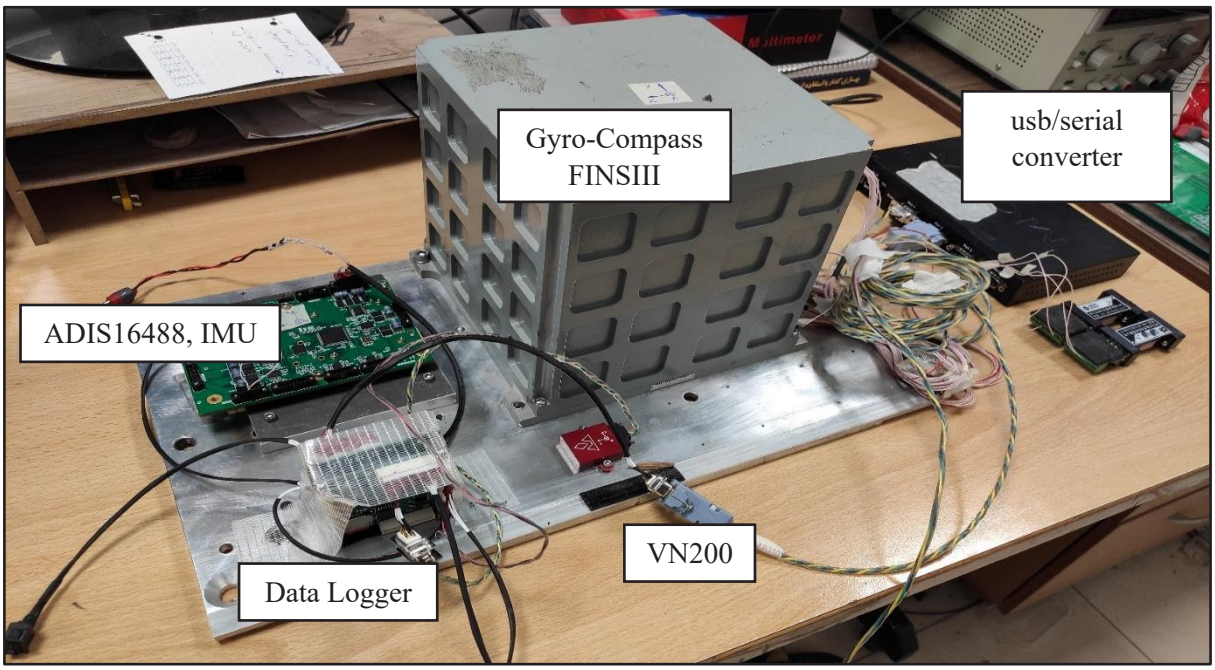

Fig. 2. Arrangement of navigation systems on the level plate to perform a car test

As seen from equation (27), the value measured by the accelerometers is equal to the gravity vector plus the term indicated by $\boldsymbol{\varepsilon}$; which is the sum of five terms: 1- Coriolis acceleration, 2- centrifugal acceleration, 3- angular acceleration, 4- linear acceleration and 5- noise.

$$\boldsymbol{\varepsilon} = 2\boldsymbol{\Omega}^{BI}(D^B\mathbf{s}_{BI}) + \boldsymbol{\Omega}^{BI}\boldsymbol{\Omega}^{BI}\mathbf{s}_{BI} + (D^B\boldsymbol{\Omega}^{BI})\mathbf{s}_{BI} + D^BD^B\mathbf{s}_{BI} + \mathbf{v} \quad (28)$$

In most vehicles, the term $\boldsymbol{\Omega}^{BI}\boldsymbol{\Omega}^{BI}\mathbf{s}_{BI}$ is larger than the two terms $2\boldsymbol{\Omega}^{BI}(D^B\mathbf{s}_{BI})$ and $(D^B\boldsymbol{\Omega}^{BI})\mathbf{s}_{BI}$,; Thus, equation (28) is approximated as follows:

$$\boldsymbol{\varepsilon} \approx \boldsymbol{\Omega}^{BI}\boldsymbol{\Omega}^{BI}\mathbf{s}_{BI} + D^BD^B\mathbf{s}_{BI} + \mathbf{v} \quad (29)$$

Assuming the terms in $\boldsymbol{\varepsilon}$ to be independent, the measurement error covariance matrix, $\mathbf{R}_{\varepsilon}$, , is obtained as follows:

$$\mathbf{R}_{\varepsilon} = \mathbf{R}_c + \mathbf{R}_l + \mathbf{R}_v \quad (30)$$

where $\mathbf{R}_v$ is the contribution of white noise; $\mathbf{R}_l$ and $\mathbf{R}_c$ are the contribution of linear and centrifugal accelerations, respectively. These Matrices are defined as follows:

$$\mathbf{R}_v = \begin{bmatrix} \sigma_{s_\theta}^2 & 0 \\ 0 & \sigma_{s_\phi}^2 \end{bmatrix} \quad (31)$$

$$\mathbf{R}_l = \alpha[|\tilde{\mathbf{a}}| - |\mathbf{g}|]^2 \quad (32)$$

$$\mathbf{R}_c = \beta|\boldsymbol{\omega}^{BI}|^4 \quad (33)$$

In equations (31), $\sigma_{s_\theta}^2$ and $\sigma_{s_\phi}^2$ are the variance of measurement error in pitch and roll angles in static conditions and are proportional to the error of the accelerometers. It is also assumed that the noise of the sensors is white with Gaussian distribution and independent from each other.

The covariance matrix of the measurement error caused by acceleration and rotation is also considered as diagonal matrices. In equation (32), the α coefficient is used for adjusting the linear acceleration error effects. Similarly, in equation (33), the β coefficient is utilized to adjust the effects of angular acceleration terms.

5- Practical test

To perform a test, three inertial navigation systems were used: 1- FINSIII gyrocompass navigation system, which, uses fiber optic gyroscopes and quartz accelerometers and can measure the alignment angles with an accuracy of hundredths of a degree; Thus, it is used as the reference. 2- The VN200 navigation system (a product of VectorNav company) is one of the most accurate attitude determination systems and is used as a comparison system. 3- The navigation system with the proposed algorithm (adaptive estimator) in which ADIS16488 is used as the inertial measurement unit. Figure 2 shows the placement of the mentioned systems in a car

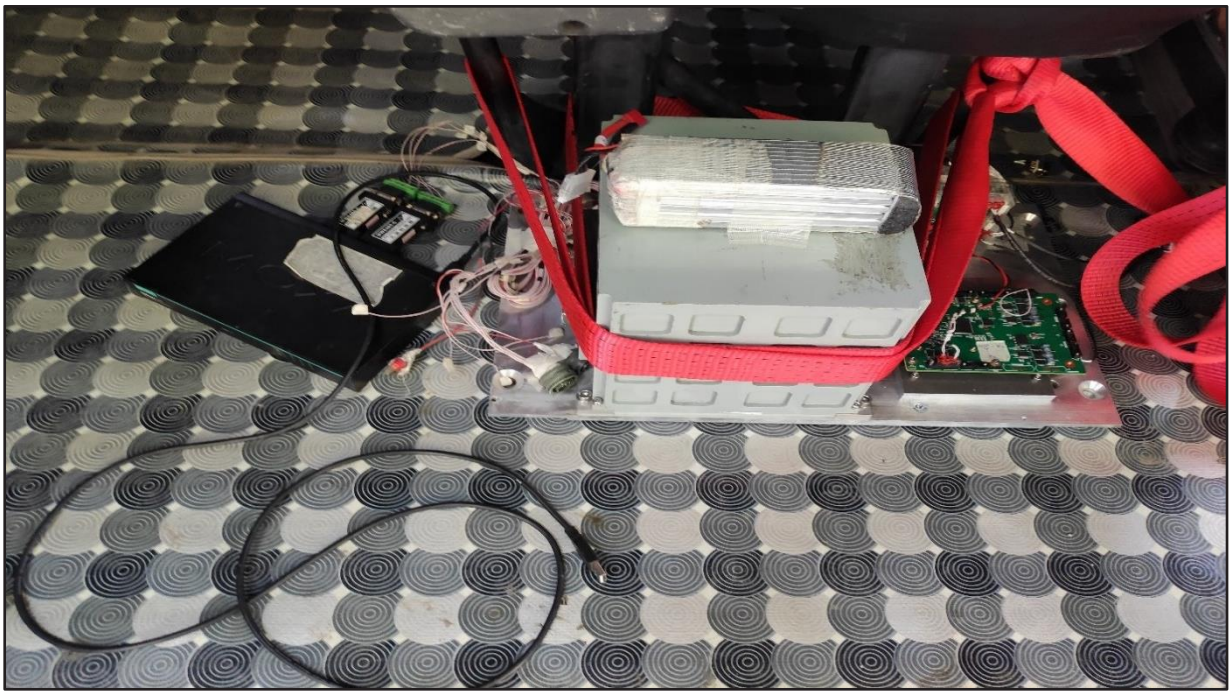

Fig. 3. Vehicle test bed

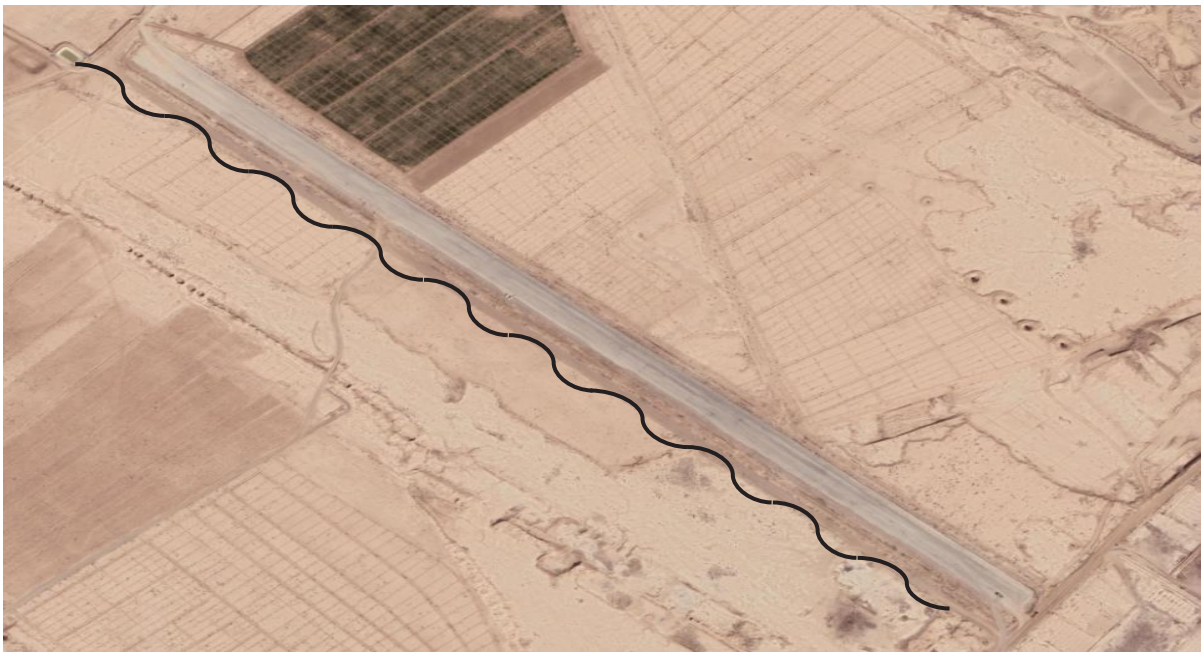

Fig. 4. Performing a spiral maneuver with the car

test. To equalize the test conditions for the three systems, a reference aluminum plate was used. The direction of the longitudinal axis of these systems was installed towards the front of the car. Figures 3 and 4 show the car test bed and the path taken during the test.

In the first scenario, the car moved at a constant speed (60 km/h). The output of accelerometers and gyros in the first scenario are shown in Figures 5 and 6 respectively. Since the car has started to move from a stationary state, it has created primary accelerations which are well seen in $\mathbf{a}_x$ accelerometer

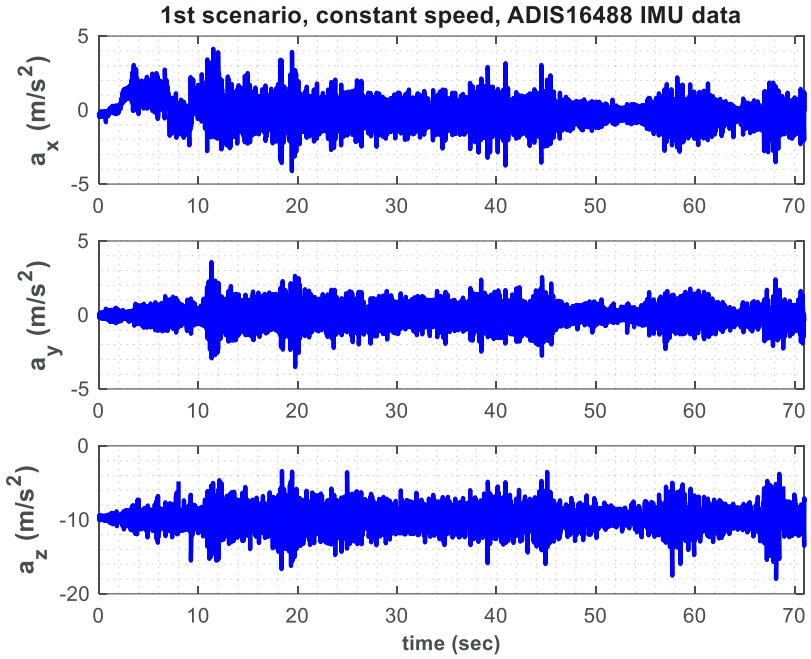

Fig. 5. Accelerometer data of ADIS16488 in constant speed movement

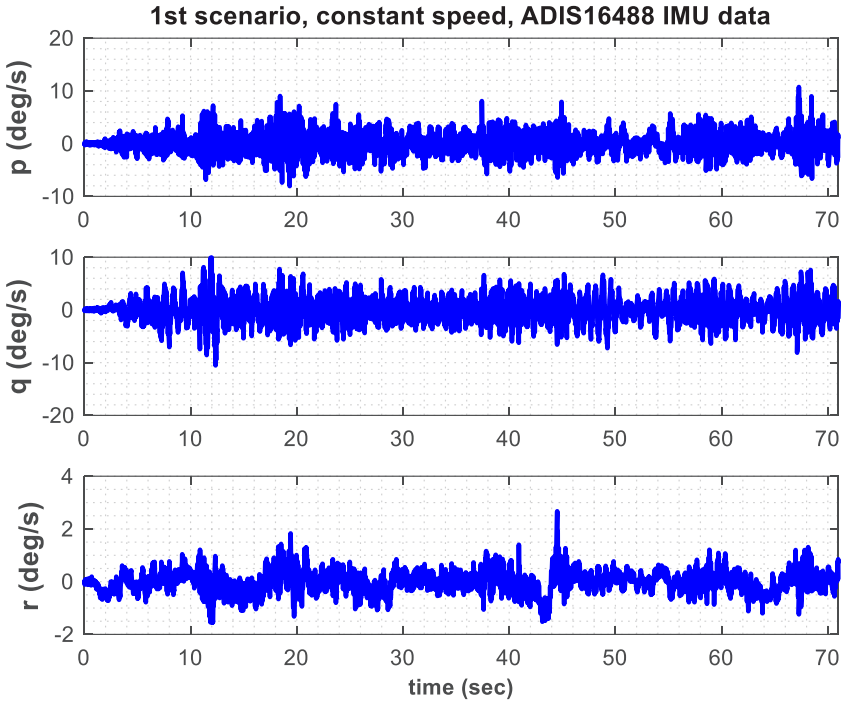

Fig. 6. ADIS16488 gyroscope data in constant speed movement

data (figure 5). The presence of these accelerations in the longitudinal direction of the car, according to equation (7) leads to an increase in the error of the pitch angle. As it is clear from Figure 7, the proposed algorithm was able to detect the accelerated movement adjust the error covariance matrix according to the maneuvering conditions, and prevent the error from increasing. In this scenario, the roll angle error variance is 0.1511 (deg^2), and the mean squared error is 0.1916 (deg^2). For the VN200 product, these numbers are 0.4691 and 0.5067, respectively. Also, in the pitch channel, the error variance for the proposed algorithm is 0.4941, and the mean square error is 0.5432. At the same time, for the VN200 product, these numbers are equal to 1.0528 and 1.1619, respectively.

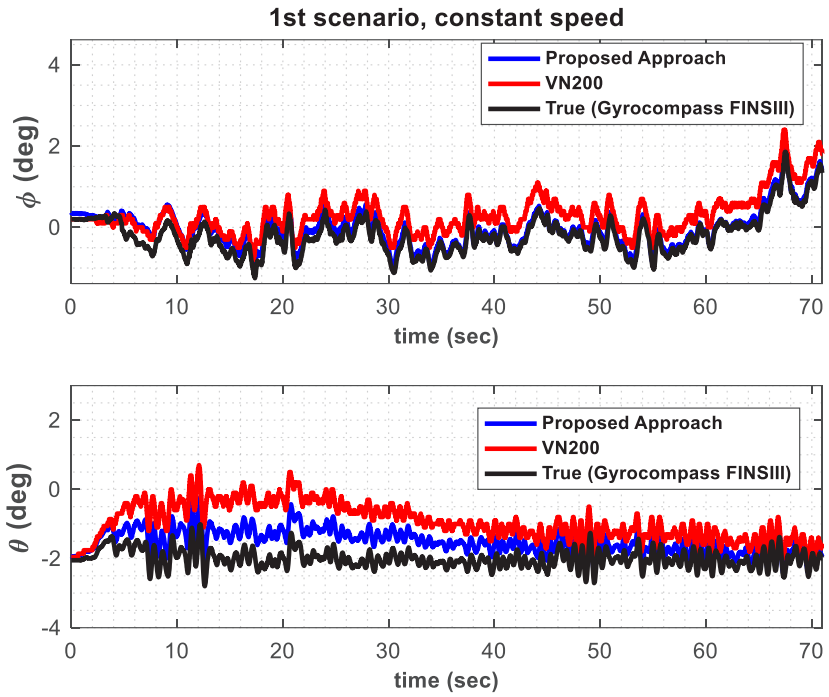

Fig. 7. Changes of alignment angles in constant speed movement

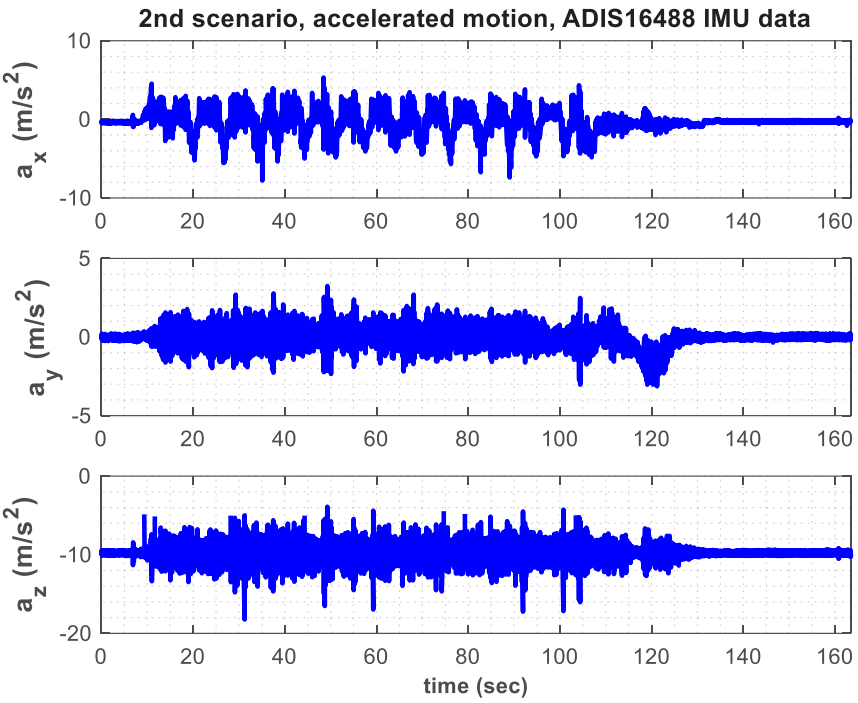

Fig. 8. Accelerometer data of ADIS16488 in accelerated motion

In the second scenario, the goal was to examine the algorithm's performance in decreasing and increasing accelerations; Therefore, by applying the gas and brake pedals successively to the car, the desired accelerations were produced. The output of accelerometers and gyros in the second scenario are shown in Figures 8 and 9 respectively. As seen in Figure 8, after pressing the gas pedal, the value of $\mathbf{a}_x$ has reached about +4m/s^2 and when the brake pedal is pressed, this value decreases to -4m/s^2. The presence of changes in longitudinal acceleration leads to an error in estimating the

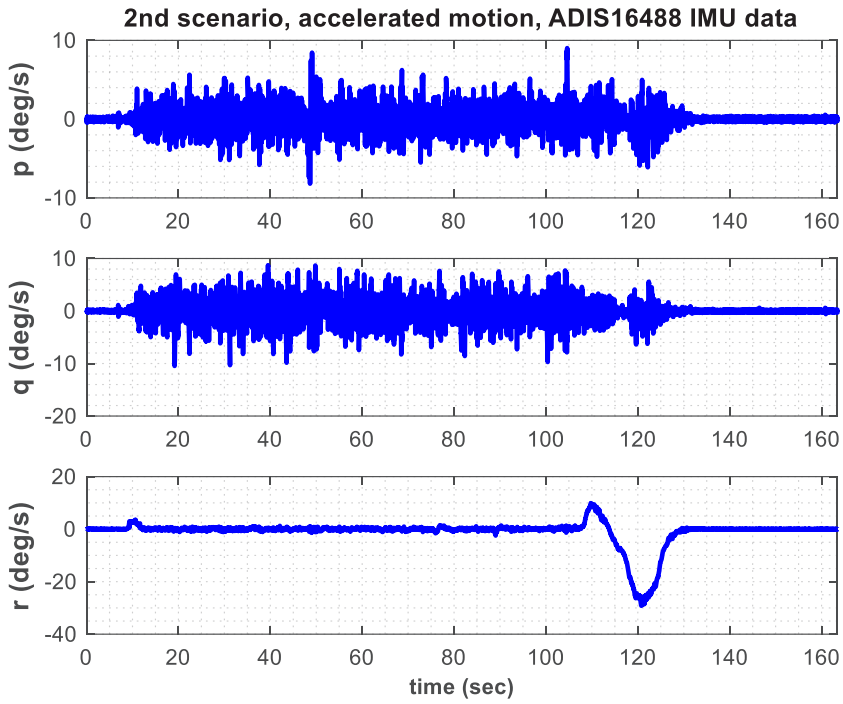

Fig. 9. ADIS16488 gyroscope data in accelerated motion

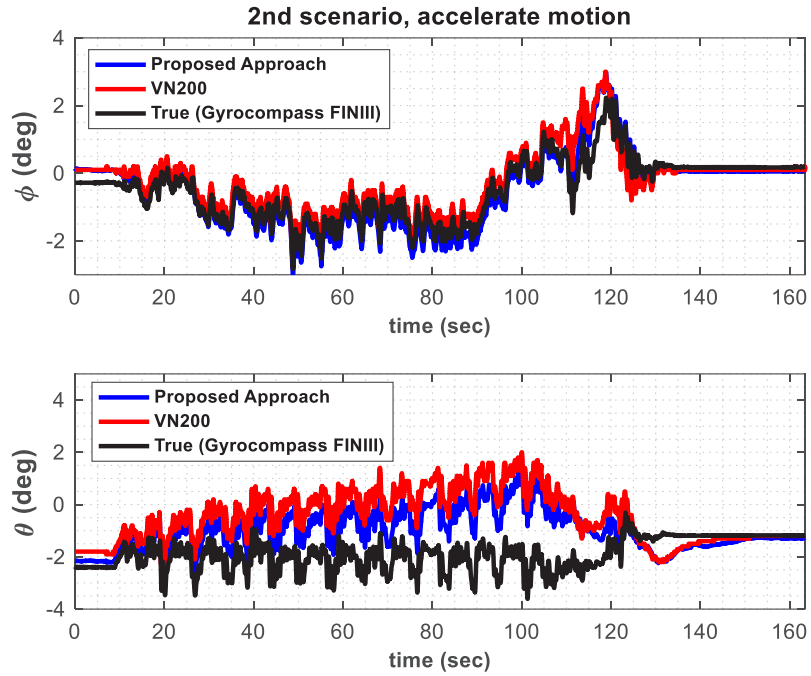

Fig. 10. Changes of alignment angles in accelerated motion

pitch angle so that within 100 seconds, three degrees of error have been created. According to Figure 10, the proposed algorithm has been able to adjust the error covariance matrix according to the existing dynamic condition and prevent the error from growing. The results in this scenario show that in the roll channel, the error variance of the proposed algorithm is 0.0431 (deg^2), and the mean square error is 0.2864 (deg^2). For the VN200 product, these numbers are 0.2502 and 0.4398, respectively. Also in the pitch channel, the variance of error for the proposed algorithm is 0.9213, and the mean square error is 1.3127; while for the VN200 product, these numbers are 1.4209 and 1.8577, respectively.

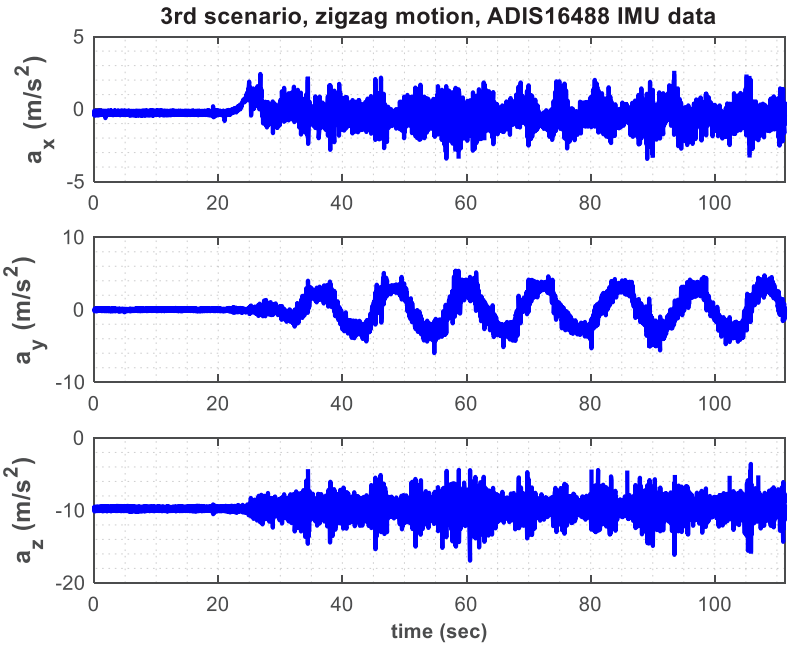

Fig. 11. Accelerometer data of ADIS16488 in spiral motion

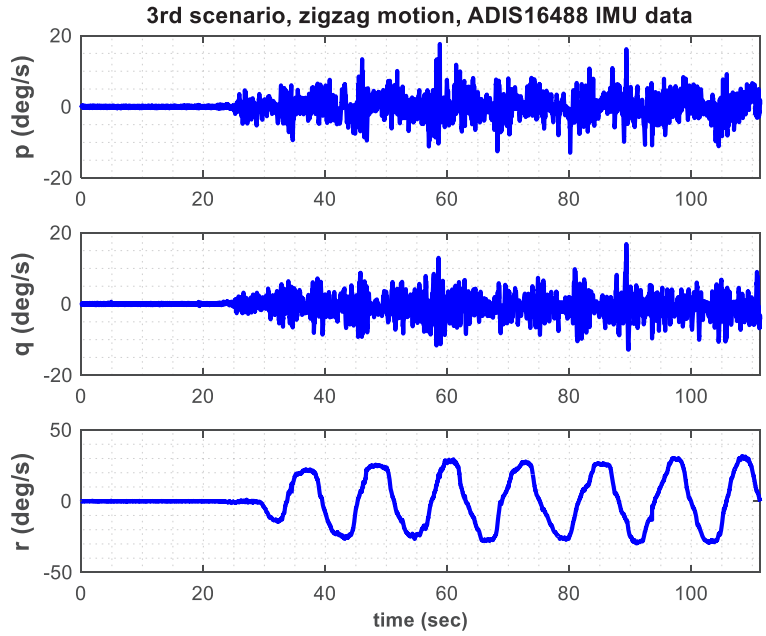

Fig. 12. ADIS16488 gyroscope data in a spiral motion

In the third scenario, to observe the effect of lateral acceleration on the performance of the algorithm, the car moved in a spiral manner. The output of accelerometers and gyros in the third scenario are shown in Figures 11 and 12 respectively. According to Figure 11, the sinusoidal changes of the acceleration in the Y axis are about 5m/s^2. The results show that although the lateral accelerations can give the car a roll angle of four to five degrees, the proposed algorithm has an acceptable accuracy in the presence of lateral accelerations. In the roll channel, the error variance of the proposed algorithm is 0.0168 (deg^2), and the mean square error is 0.2065 (deg^2). For the VN200 product, these

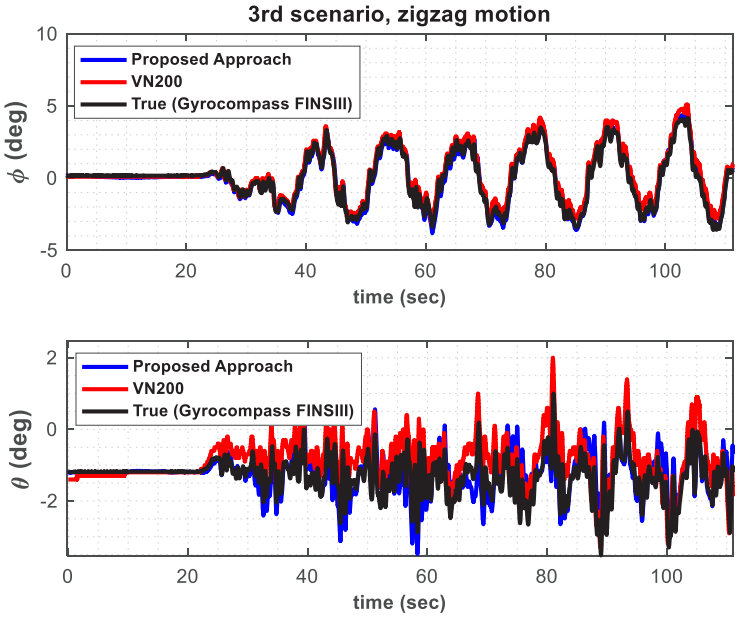

Fig. 13. Changes of alignment angles in a spiral movement

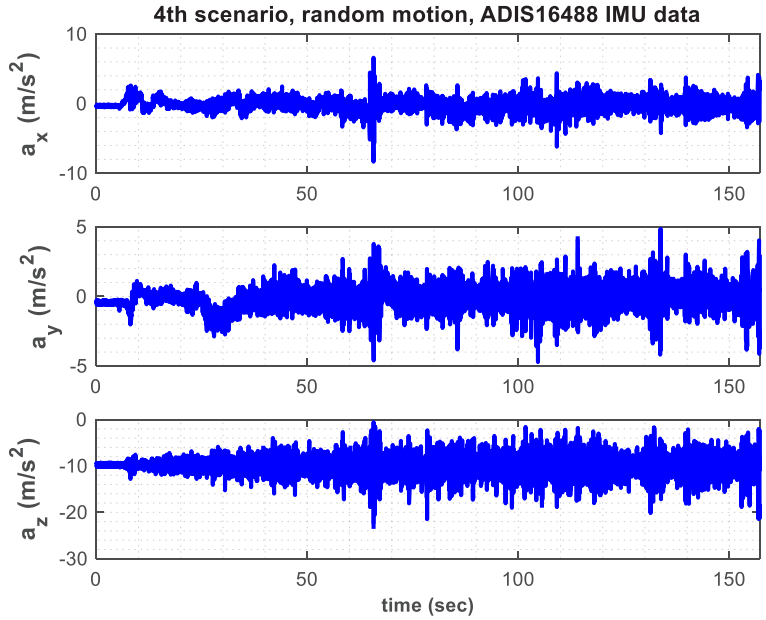

Fig. 14. ADIS16488 accelerometer data in random motion

numbers are 0.2948 and 0.4644, respectively. Also, in the pitch channel, the error variance of the proposed algorithm is 0.0657, and the mean squared error is 0.3762; While, for the VN200 product, these numbers were 0.4025 and 0.5760, respectively.

In the fourth scenario, the car's movement was done randomly so that all the maneuvering conditions were put together. The output of accelerometers and gyros in the fourth scenario are shown in Figures 14 and 15 respectively. The fourth scenario started with the car turning at the beginning of the route. Then the movement continued in an accelerated manner. After that, sudden acceleration was applied to the system after passing an obstacle. The accuracy of the algorithm in the roll channel is better than the pitch one. The performance of the proposed algorithm was acceptable when crossing the obstacle. The results of this scenario show

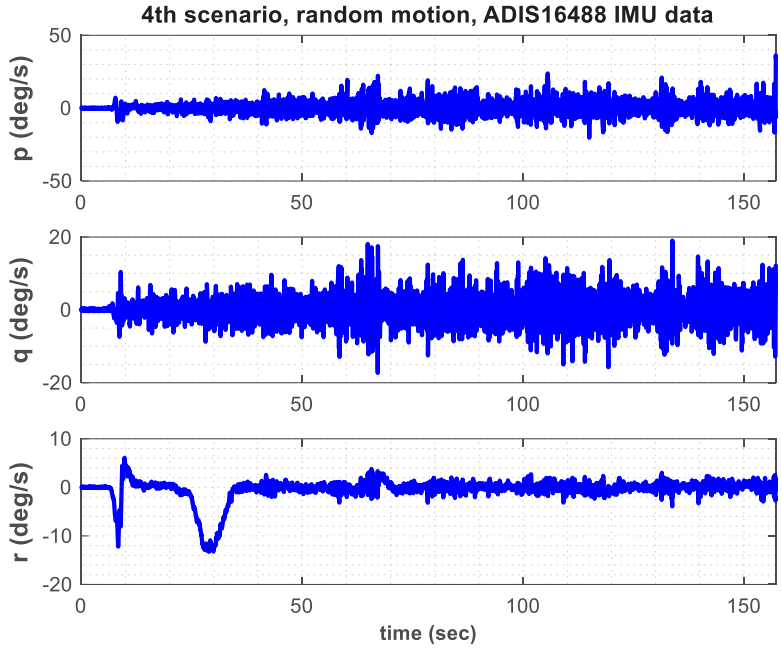

Fig. 15. ADIS16488 gyroscope data in random motion

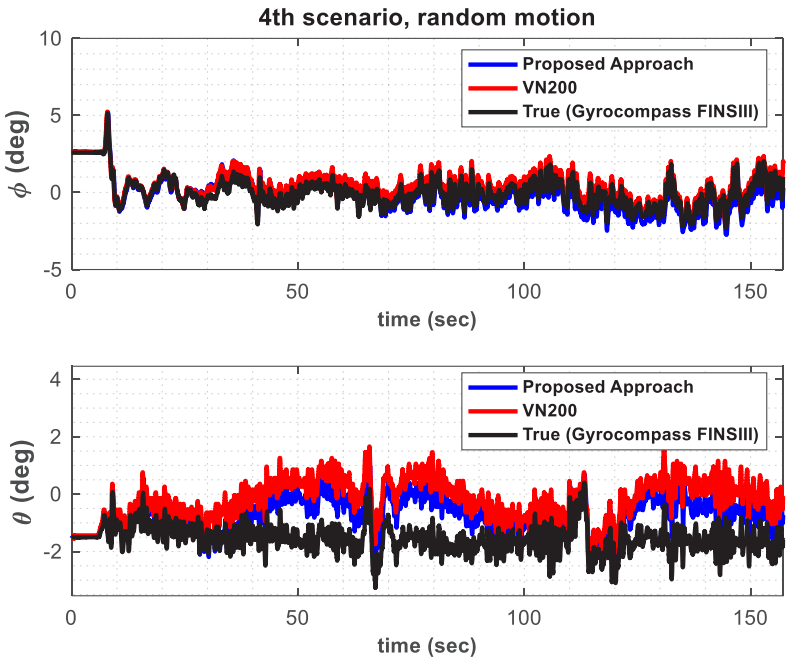

Fig. 16. Changes of alignment angles in random motion

that in the roll channel, the error variance is 0.1337 (deg^2), and the mean square error is 0.4024 (deg^2). For the VN200 product, these numbers are 0.4116 and 0.4923, respectively. Also, in the pitch channel, the error variance of the proposed algorithm is 0.8562, and the mean square error is 1.0063; while for the VN200 product, these numbers are 1.3223 and 1.4827, respectively. Tables 1-2 show the performance of the proposed Adaptive Estimator Algorithm (AEA) compared to the VN200 product.

Table 1. Comparing the performance of the adaptive estimator algorithm with the Vn200 product in determining the roll angle

Movement Phase	Sum of Squared Error		Error Variance	
	Vn200	AEA	Vn200	**AEA**
Constant Speed	0.5067	0.1916	0.4691	**0.1511**
Accelerated	0.4398	0.2864	0.2502	**0.0431**
Spiral	0.4644	0.2065	0.2948	**0.0168**
Random	0.4923	0.4024	0.4116	**0.1337**

Table 2. Comparing the performance of the adaptive estimator algorithm with the Vn200 product in determining the pitch angle

Movement Phase	Sum of Squared Error		Error Variance	
	Vn200	AEA	Vn200	**AEA**
Constant Speed	1.1619	0.5432	1.0528	**0.4941**
Accelerated	1.8577	1.3127	1.4209	**0.9213**
Spiral	0.5760	0.3762	0.4025	**0.0657**
Random	1.4827	1.0063	1.3223	**0.8562**

6- Conclusion

In this paper, a new analytical-comparative method was proposed to determine the attitude using a three-axis accelerometer and gyroscope sensors. The proposed algorithm does not use the navigation aiding data to estimate the attitude. For this purpose, by expanding the analytical equations in rotational kinematics of a rigid body, the comparative values of the measurement covariance matrix were extracted in such a way that despite the external accelerations applied to the body, an accurate estimate of level angles was obtained. The simulation results, along with the vehicle tests that were performed in different dynamic conditions, showed that the proposed algorithm has a high ability to estimate the level angles accurately.

References

[1] 2017, Comparison of Complementary and Kalman Filter Based Data fusion for attitude Heading Reference System

[2] 2019, A Robust Complementary Filter Approach for Attitude Estimation of Unmanned Aerial Vehicles using AHRS

[3] A Complementary Filter for Attitude Estimation

[4] 2021, Attitude Adaptive Estimation with Smart Phone Classification for Pedestrian Navigation.

[5] Crassidis, J. L., and Junkins, J. L. Optimal Estimation of Dynamic Systems. Chapman and Hall/CRC, 2011.

[6] Jazwinski, A. H. Stochastic Processes, and Filtering Theory. Courier Corporation, 2007.

[7] Schmidt, S. F. "The Kalman Filter-Its Recognition and Development for Aerospace Applications." Journal of Guidance and Control, Vol. 4, No. 1, 1981, pp. 4–7.

[8] Farrell, J. L. "Attitude Determination by Kalman Filtering." Automatica, Vol. 6, No. 3, 1970, pp. 419–430.

[9] Murrell, J. Precision Attitude Determination for Multimission Spacecraft. 1978.

[10] Lefferts, E. J., Markley, F. L., and Shuster, M. D. "Kalman Filtering for Spacecraft Attitude Estimation." Journal of Guidance, Control, and Dynamics, Vol. 5, No. 5, 1982, pp. 417–429.

[11] Markley, F. L. "Attitude Error Representations for Kalman Filtering." Journal of guidance, control, and dynamics, Vol. 26, No. 2, 2003, pp. 311–317.

[12] Bar-Itzhack, I. Y., and Oshman, Y. "Attitude Determination from Vector Observations: Quaternion Estimation." IEEE Transactions on Aerospace and Electronic Systems, No. 1, 1985, pp. 128–136.

[13] Bar-Itzhack, I., Deutschmann, J., and Markley, F. Quaternion Normalization in Additive EKF for Spacecraft Attitude Determination. 1991.

[14] Deutschmann, J., Bar-Itzhack, I., and Galal, K. Quaternion Normalization in Spacecraft Attitude Determination. 1992.

[15] Psiaki, M. L., Theiler, J., Bloch, J., Ryan, S., Dill, R. W., and Warner, R. E. "ALEXIS Spacecraft Attitude Reconstruction with Thermal/Flexible Motions Due to Launch Damage." Journal of Guidance, Control, and Dynamics, Vol. 20, No. 5, 1997, pp. 1033–1041.

[16] Psiaki, M. L., Klatt, E. M., Kintner Jr, P. M., and Powell, S. P. "Attitude Estimation for a Flexible Spacecraft in an Unstable Spin." Journal of Guidance, Control, and Dynamics, Vol. 25, No. 1, 2002, pp. 88–95.

[17] Choukroun, D., Bar-Itzhack, I. Y., and Oshman, Y. "Novel Quaternion Kalman Filter." IEEE Transactions on Aerospace and Electronic Systems, Vol. 42, No. 1, 2006, pp. 174–190.

[18] Psiaki, M. L. "Backward-Smoothing Extended Kalman Filter." Journal of guidance, control, and dynamics, Vol. 28, No. 5, 2005, pp. 885–894.

[19] Landis Markley, F., Berman, N., and Shaked, U. "H -Type Filter for Spacecraft Attitude Estimation." ADVANCES IN THE ASTRONAUTICAL SCIENCES, Vol. 84, 1994, p. 697.

[20] Markley, F. L., Berman, N., and Shaked, U. Deterministic EKF-like Estimator for Spacecraft Attitude Estimation. No. 1, 1994, pp. 247–251.

[21] Smith, R. H. "An H1-Type Filter for GPS-Based Attitude Estimation." AAS Paper, 1995, pp. 95–134.

[22] Haupt, G. T., Kasdin, N. J., Keiser, G. M., and Parkinson, B. W. "Optimal Recursive Iterative Algorithm for Discrete Nonlinear Least-Squares Estimation." Journal of guidance, control, and dynamics, Vol. 19, No. 3, 1996, pp. 643–649.

[23] Mehra, R. "On the Identification of Variances and Adaptive Kalman Filtering." IEEE Transactions on automatic control, Vol. 15, No. 2, 1970, pp. 175–184.

[24] Ma, Z., and Ng, A. Spacecraft Attitude Determination by Adaptive Kalman Filtering. 2002.

[25] Lam, Q. M., and Wu, A. Enhanced Precision Attitude Determination Algorithms. No. 1, 1998, pp. 61–68.

[26] Mehra, R., Seereeram, S., Bayard, D., and Hadaegh, F. Adaptive Kalman Filtering, Failure Detection and Identification for Spacecraft Attitude Estimation. 1995.

[27] Rapoport, I., and Oshman, Y. Optimal Filtering in the Presence of Faulty Measurement Biases. No. 2, 2002, pp. 2236–2241.

[28] Carter, M., Vadali, S., Chamitoff, G., Carter, M., Vadali, S., and Chamitoff, G. Parameter Identification for the International Space Station Using Nonlinear Momentum Management Control. 1997.

[29] Kim, J.-W., Crassidis, J. L., Vadali, S. R., and Dershowitz, A. L. International Space Station Leak Localization Using Vent Torque Estimation. 2004.

[30] Psiaki, M. L. Estimation of the Parameters of a Spacecrafts Attitude Dynamics Model Using Flight Data. 2003.

[31] Kim, I., Kim, J., and Kim, Y. Angular Rate Estimator Using Disturbance Accommodation Technique. 2002.

[32] Schaub, H., Akella, M. R., and Junkins, J. L. "Adaptive Control of Non-linear Attitude Motions Realizing Linear Closed Loop Dynamics." Journal of Guidance, Control, and Dynamics, Vol. 24, No. 1, 2001, pp. 95–100.

[33] Costic, B. T., Dawson, D. M., De Queiroz, M. S., and Kapila, V. "Quaternion-Based Adaptive Attitude Tracking Controller without Velocity Measurements." Journal of Guidance, Control, and Dynamics, Vol. 24, No. 6, 2001, pp. 1214–1222.

[34] 1997, Inertially Aided GPS Based Attitude Heading Refrence system AHRS for general aviation aircraft

[35] M. Ncørguard, N. K. Poulsen, O. Ravn, New developments in state estimation for non-linear systems, Journal of Automatica, Vol. 36, No. 11, pp. 1627-1638, 2000.

[36] Lefferts, E. J., Markley, F. L., and Shuster, M. D., "Kalman Filtering for Spacecraft Attitude Estimation", Journal of Guidance, Control, and Dynamics, Vol. 5, No. 5, 1982, pp. 417–429.

[37] Markley, F. L., "Attitude Error Representations for Kalman Filtering," Journal of Guidance, Control, and Dynamics, Vol. 63, No. 2, 2003, pp. 311–317.

[38] Yan, Z., Li, B., & Zhu, S. (2020). "Improved AHRS Algorithm for Unmanned Aerial Vehicles Based on Particle Filter. " Sensors, 20(21), 6253.

[39] Zhang, R., Wei, X., & Ma, J. (2020). "A Novel Inertial Navigation System Using a Low-Cost MEMS AHRS." Sensors, 20(24), 7256.

[40] Zhou, H., Wang, F., & Zhang, Z. (2021). "Adaptive Unscented Kalman Filter for Improving Attitude Estimation Accuracy of MEMS-Based AHRS." Sensors, 21(2), 503.

[41] Delgado-Mata, C., De Sousa, R. A., & Fu, W. (2021). "Novel Adaptive Unscented Kalman Filter with Fading Memory for Robust AHRS." IEEE Sensors Journal, 21(14), 15262-15273.

[42] Liu, X., Zhang, T., & Lv, P. (2021). "Attitude Estimation for AHRS Based on Mahony Filter and Adaptive Notch Filter." In 2021 7th International Conference on Control, Automation and Robotics (ICCAR) (pp. 692-697). IEEE.

[43] Hovland, G., Børhaug, T. E., & Johansen, T. A. (2021). "Nonlinear Optimization of the Attitude and Heading Reference System Problem." Journal of Guidance, Control, and Dynamics, 44(11), 2236-2249.

[44] Zeng, J., Liu, Y., & Han, C. (2022). "AHRS Correction Algorithm Based on RBF Neural Network for Underwater AUVs." IEEE Access, 10, 36399-36411.

[45] Shu, X., Li, H., & Zhu, L. (2022). "Quaternion-Based Adaptive Unscented Kalman Filter for AHRS with Biased Rate Gyro." IEEE Transactions on Instrumentation and Measurement, 71, 1-12.

[46] Li, T., & Liu, H. (2022). "A Robust AHRS Attitude Complementary Filter Algorithm Based on a Nonlinear Parameter Fading Extended Kalman Filter." IEEE Access, 10, 72988-72998.

[47] Wu, J., Gao, Y., & Liu, H. (2022). "Adaptive Unscented Kalman Filter Algorithm for Attitude and Heading Reference System." IEEE Access, 10, 23157-23165.

[48] 2007, Calibration and data fusion solution for the miniature attitude and heading reference system

[49] 2020, Attitude heading reference algorithm based on transformed cubature Kalman filter

[50] 2020, Attitude determination improvement in accelerated motions for maneuvering underwater vehicles

[51] 2014, Accurate orientation estimation using AHRS under conditions of magnetic distortion

[52] Adaptive filter for a miniature MEMS based attitude and heading reference system, 2004.

[53] 2020, Fuzzy Adaptive Attitude Estimation for a Fixed-Wing UAV with a Virtual SSA

[54] Sensor During a GPS Outage

[55] 2021, A novel adaptive Kalman filter for Euler-angle-based MEMS IMU/magnetometer attitude estimation

[56] 2018, Kalman filter for mobile-robot attitude estimation: Novel optimized and adaptive solutions

[57] Peter H. Zipfel, Modeling and Simulation of Aerospace Vehicle Dynamics, 2000

[58] Dan. Simon

HOW TO CITE THIS ARTICLE

M.A. Amiri Atashgah, M. Ebrahimi Dormiani,H. Mohammadkarimi, A Robust Self-contained Solution for Inertial Attitude Determination Under External Acceleration. AUT J. Model. Simul., 55(1) (2023) 183-198.

DOI: 10.22060/miscj.2023.22582.5332